arXiv:1510.05158v1 [astro-ph.EP] 17 Oct 2015

Distributions of Long-Lived Radioactive Nuclei Provided by Star Forming Environments

Marco Fatuzzo

Department of Physics, Xavier University, Cincinnati, OH 45207

and

Fred C. Adams

Physics Department, University of Michigan, Ann Arbor, MI 48109

ABSTRACT

Radioactive nuclei play an important role in planetary evolution by providing an internal heat source, which affects planetary structure and helps facilitate plate tectonics. A minimum level of nuclear activity is thought to be necessary — but not sufficient — for planets to be habitable. Extending previous work that focused on short-lived nuclei, this paper considers the delivery of long-lived radioactive nuclei to circumstellar disks in star forming regions. Although the long-lived nuclear species are always present, their abundances can be enhanced through multiple mechanisms. Most stars form in embedded cluster environments, so that disks can be enriched directly by intercepting ejecta from supernovae within the birth clusters. In addition, molecular clouds often provide multiple episodes of star formation, so that nuclear abundances can accumulate within the cloud; subsequent generations of stars can thus receive elevated levels of radioactive nuclei through this distributed enrichment scenario. This paper calculates the distribution of additional enrichment for ^{40}K, the most abundant of the long-lived radioactive nuclei. We find that distributed enrichment is more effective than direct enrichment. For the latter mechanism, ideal conditions lead to about 1 in 200 solar systems being directly enriched in ^{40}K at the level inferred for the early solar nebula (thereby doubling the abundance). For distributed enrichment from adjacent clusters, about 1 in 80 solar systems are enriched at the same level. Distributed enrichment over the entire molecular cloud is more uncertain, but can be even more effective.

Subject headings: open clusters and associations: general - planets and satellites: formation - planet - star interactions - stars: formation

1. Introduction

The chemical composition of circumstellar disks is important both for their evolution and for the properties of the planets they ultimately produce. In previous work, a great deal of attention

has been given to the short-lived radioisotopes (SLRs), such as ^{26}Al and ^{60}Fe (e.g., see the results from Cameron & Truran 1977 to Mishra & Goswami 2014). Meteoritic evidence indicates that the early solar system was enriched in several species of SLRs, especially ^{26}Al, and these nuclei provide vital sources of both heating and ionization to the early solar nebula and other planet-forming disks (Cleeves et al. 2013; Umebayashi & Nakano 2009). In addition, as outlined below, long-lived radioisotopes (LLRs) can also play an important role in the long-term evolution of planets. Whereas SLRs decay quickly and their inventory in disks must be produced locally, LLRs have a baseline contribution from the background nuclear supply of the galaxy. On the other hand, LLRs are produced via supernovae (e.g., Mathews et al. 1992; Timmes et al. 1995), which are often associated with star forming regions. As a result, these supernovae can enrich nearby circumstellar disks with an extra complement of LLRs (in addition to the LLRs present in the original molecular cloud material). The goal of this paper is to quantify the additional enrichment of disks with LLRs due to supernovae in star forming regions.

The chemical composition of the disk is important not only for planet formation in general, but also for the formation of habitable planets in particular. The most basic requirements for habitability are often taken to be [1] the planetary mass is comparable to Earth, and [2] the stellar insolation is comparable to that received on Earth so that the planet can retain liquid water on its surface over geologically interesting time scales (Kasting et al. 1993; Lunine 2005; Scharf 2009). Moving beyond these basic necessities, many authors have suggested that habitable planets require additional chemical constraints (Kasting et al. 1993; Gonzalez et al. 2001). As one example, an important variable for the formation of planets is the surface density of solid material in the disk, so that planet formation is favored in systems with high metallicity. On the other hand, recent results indicate that terrestrial planet formation is not as sensitive to metallicity as the formation of larger bodies (Buchave et al. 2012). Moreover, habitability is thought to require a sufficient level of geological activity (Frank et al. 2014), including interior heat production and crustal recyling (e.g., active plate tectonics). This activity is enhanced by LLRs such as ^{40}K, ^{235}U, ^{238}U, and ^{232}Th. Of these, ^{40}K is the most abundant and best understood. In contrast, the actinides are produced solely via the r-process. While the conditions necessary for the functioning of the r-process are well understood, theoretical models fail to produce the full gamut of r-nuclides expected. As such, uncertainty remains as to both the mechanism and astrophysical site of actinide production. We therefore focus solely on the delivery of ^{40}K to circumstellar disks in their early evolutionary phases.

Radioactive nuclei can be delivered to planet-forming disks through two conceptually different mechanisms. In the direct enrichment scenario, supernovae explode within the birth cluster and provide radioactive nuclei to any circumstellar disks that are favorably positioned at the time of detonation. This channel of enrichment is important for SLRs; because of their short half-lives, SLRs must be incorporated into disks on short time scales. In previous work (Adams et al. 2014; hereafter Paper I), we found the distributions of SLR abundances provided to solar systems through this channel of enrichment. Clusters can account for the abundances of SLRs inferred for our solar system, but only $\sim 10\%$ of the time; typical enrichment levels are 10 times lower.

As star formation continues, radioactive nuclei are injected into the background molecular cloud, where they are available to enrich the next generation of stars and disks (Gounelle & Meibom 2008; Gounelle et al. 2009). This distributed enrichment process can compete with direct enrichment for the case of SLRs. In this paper, we explore both the direct and distributed enrichment scenarios for the case of long-lived radioisotopes. We find that distributed enrichment is more effective than direct enrichment for the LLRs, as expected. However, a small fraction of solar systems (of order 1%) can experience substantial enrichment, through either mechanism. As a result, a small fraction of potentially habitable planets are predicted to have radioactive complements that exceed that of Earth. Although the fraction is low, the total number of such planets in our Galaxy could still number in the billions.

This paper is organized as follows. In §2 we review the nuclear yield for ^{40}K, and obtain IMF averaged values under various scenarios. The resulting enrichment levels for direct injection of nuclei into disks within a cluster environment are presented in §3. We present distributions of enhancements for individual solar systems for a distribution of clusters that mimics the observed local cluster distribution, and also a distribution of clusters that extends up to 10^6 members. We consider cases of distributed enrichment in §4, which presents results of a neighboring cluster enrichment scenario, and develops a model of radioactive abundances over the lifetimes of molecular clouds. For both the direct enrichment scenario (§3) and the case of enrichment by neighboring clusters (§4.1), the abundances of ^{40}K are determined by a straightforward (but complicated) accounting calculation, and can be directly compared; for the case of distributed enrichment over the whole molecular cloud, however, we present only a simple model, which contains more uncertainties (see §4.2). The paper concludes, in §5, with a summary of the results and a discussion of their implications for the formation of habitable planets.

2. Abundance and Nuclear Yields for ^{40}K

The abundance of elements throughout the Milky Way represents a fundamental field in astronomy that informs our understanding of stellar evolution, Galactic chemical evolution, and planet formation. Perhaps not surprisingly, variations in elemental abundances have been observed in nearby F and G stars in the Galactic thin disk (e.g., Reddy et al. 2003), and abundances generally decrease with galactocentric radius. For purposes of our investigation, we use early (4.56 Gyrs ago) solar system abundances as derived from chondritic meteorites and the solar photosphere to help guide the analysis of our results (Lodders 2010). Those values normalized to 10^6 Si atoms are presented in Table 1 for the most active long-lived radioactive isotopes, along with corresponding half-lifes $t_{1/2}$ and relative activity $\dot{N}_S \equiv \lambda N_S$ (where $\lambda = \ln[2]/t_{1/2}$). In addition to ^{40}K, we include for comparison the parameters for Uranium and Thorium; note that their relative activity is much lower than that of ^{40}K.

The production of ^{40}K occurs primarily in the supernova events that mark the death of massive stars. Detailed calculations of nucleosynthesis yields of this isotope as a function of progenitor star

mass appear in the seminal paper by Woosley & Weaver (1995 - hereafter WW95) and the follow up paper by Rauscher et al. (2002 - hereafter R02), although the latter does so for a narrower 15 – 25 $M_\odot$ mass range. We therefore update the ^{40}K yields presented in WW95 (which spans 8 – 40 $M_\odot$) with those presented in R02 over the 15 - 25 $M_\odot$ range. In order to get yields for any specified mass above the supernova threshold of 8 $M_\odot$, we adopt a linear interpolation scheme in log-log space, and extrapolate from the endpoint values down to $8M_\odot$ and up to an assumed maximum stellar mass of $120M_\odot$. Yield rates and interpolated/extrapolated values are presented in Figure 1. Although our analysis incorporates yields calculated for progenitor stars with solar metallicity, stellar evolution could affect our results. Toward that end, we note that WW95 calculate yields for progenitor stars for different metallicities $Z/Z_\odot$. We present their full results for ^{40}K in Figure 2.

We next consider the yield per star expected from a population of stars born with a specified initial mass function (IMF). Following Adams et al. (2014), we parametrize the high mass portion of the stellar IMF that leads to supernova events through the power-law relation

$$\frac{dN_*}{dm} = \mathcal{F}_{\rm SN} \, \frac{\gamma}{8} \left(\frac{m}{8} \right)^{-(\gamma+1)} \ , \tag{1}$$

where $\mathcal{F}_{\rm SN}$ is the fraction of the (initial) stellar population with mass greater that the minimum mass $m_{min} = 8$ (in solar units) required for a star to end its life with a supernova explosion, m is the stellar mass in solar units, and γ is an index value. From observations, we expect $F_{SN} \approx 0.005$ (e.g., Adams & Fatuzzo 1996; Kroupa 2001; Chabrier 2003) and $\gamma \approx 1.35$ (e.g., Salpeter 1955). But given the observed scatter in the index γ along with its observational uncertainty, we consider a range of $1 \leq \gamma \leq 2$ in our analysis. Note that the relation given in Equation (1) is normalized so that

$$\int_8^\infty \frac{dN_*}{dm} \, dm = \mathcal{F}_{\rm SN} \ , \tag{2}$$

and thus requires a correction factor of $f_C = [1 - (8/m_\infty)^\gamma]$ for an IMF with an upper mass limit m_∞. This correction factor is $f_C = 0.983$ for a fiducial value of $m_\infty = 120$ and an index $\gamma = 1.5$, and since a ~ 2 percent correction is much smaller than the other uncertainties in the problem, we will generally ignore it.

The yield per star weighted by a stellar IMF with index γ is then found through the integral

Table 1. Table of long-lived nuclear isotopes

Isotope	$t_{1/2}$ (Gyrs)	N_s	$\dot{N}_s$ (Gyrs^{-1})
^{40}K	1.25	6	3.3
^{232}Th	14.1	0.0440	0.0022
^{238}U	4.47	0.0180	0.0028
^{235}U	0.704	0.0058	0.0057

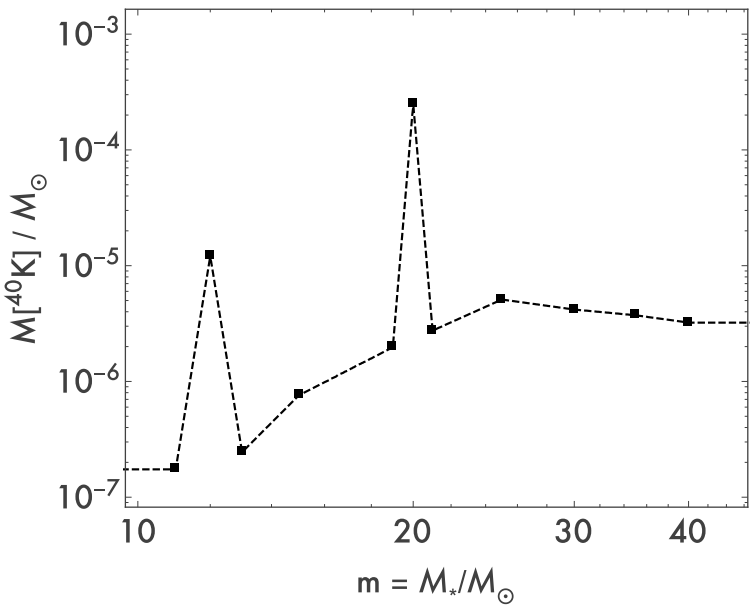

Fig. 1.— Calculated radioactive yield $M[^{40}\mathrm{K}]$ as a function of progenitor mass M_* based on the results from WW95 and R02. The dashed line represents the adopted interpolation / extrapolation scheme as outlined in the text of the paper.

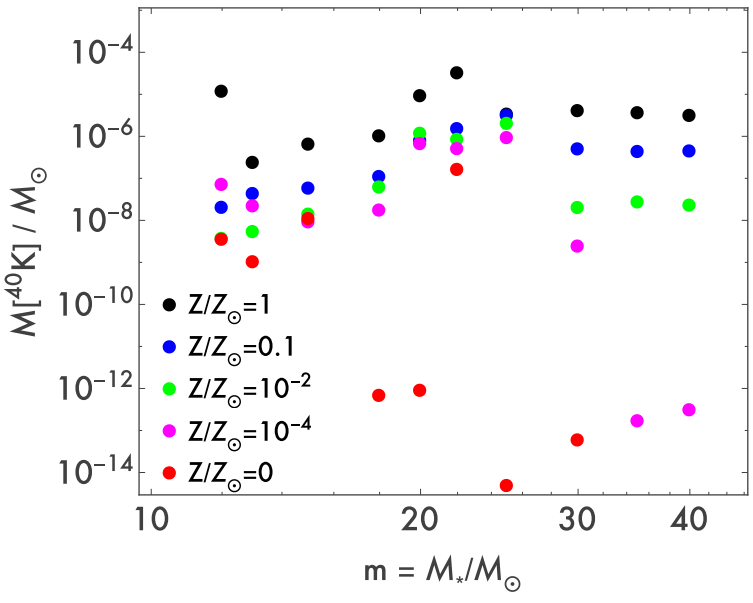

Fig. 2.— Calculated radioactive yield $M[^{40}\mathrm{K}]$ as a function of progenitor mass for several metallicities (Woosley and Weaver 1995).

expression

$$\langle M[^{40}\mathrm{K}]\rangle_* \equiv \int_8^\infty M[^{40}\mathrm{K}; m]\frac{dN_*}{dm}\,dm\,, \tag{3}$$

where $M[^{40}\mathrm{K}; m]$ is the yield of ^{40}K as a function of progenitor mass m (as illustrated by the dashed line in Figure 1 for our adopted interpolation/extrapolation scheme). The yield per star for ^{40}K is shown in Figure 3 as a function of γ. Note that the yield per supernova weighted by a stellar IMF with index γ is given by the relation

$$\langle M[^{40}\mathrm{K}]\rangle_{SN} = \frac{\langle M[^{40}\mathrm{K}]\rangle_*}{\mathcal{F}_{SN}}\,. \tag{4}$$

The "background" value for ^{40}K as defined by its number ratio to hydrogen $(N_{^{40}\mathrm{K}}/N_H)_{BG}$ can be estimated by assuming a uniform mixing of SN ejecta with the interstellar medium. Adopting a constant fiducial rate $\mathcal{R}_{SN} = 0.01$ yr^{-1} of supernova events, constant yields obtained using an IMF index of $\gamma = 1.5$ and solar metallicity, and using a fiducial value of $M_H = 5.5 \times 10^9 M_\odot$ for the hydrogen mass in the ISM, the steady-state abundance $M[^{40}\mathrm{K}]_0$ is easily found by balancing the injection and decay rates

$$\mathcal{R}_{SN}\langle M[^{40}\mathrm{K}]\rangle_{SN} = \lambda M[^{40}\mathrm{K}]_0\,, \tag{5}$$

which then yields a value of $(N_{^{40}\mathrm{K}}/N_H)_{BG} = 2.8\times10^{-10}$. In contrast, the early solar system value is $(N_{^{40}\mathrm{K}}/N_H)_{SS} = 2.3 \times 10^{-10}$ (Lodders 2010). We note that our idealized analysis ignores evolution effects both in the rate of supernovae and the yields (which are strongly dependent on metallicity Z as shown in Figure 2). In addition, a significant fraction of the isotope mass is likely locked up in stars and stellar remnants. In all, our estimate is therefore likely an upper limit to the actual value.

3. Cluster Self–Enrichment Distributions

We consider first a scenario where enrichment occurs within a cluster due to its own members. In this case, only the most massive stars would evolve on short enough timescales to affect disk evolution. Specifically, circumstellar disks are expected to retain their gas for $\sim 3 - 10$ Myrs, and only $M_* \gtrsim 16 M_\odot$ stars evolve all the way to core-collapse on comparable timescales. As a way of quantifying how stellar evolution affects the yield of long-lived radioactive isotopes within a single cluster, we calculate nuclear yields per star for different values of m_{min} of a parent IMF with spectral index $\gamma = 1.5$. As shown in Figure 4, the yields (per star) of ^{40}K, which decreases steadily with increasing minimum mass, is fairly sensitive to m_{min}, and hence to cluster and stellar disk evolution within a cluster environment. To further illustrate this point, we plot in Figure 5 the nuclear yield (per star) of ^{40}K as a function of cluster age τ assuming that only stars that have evolved to core-collapse are included in the yield - that is, we match the cluster age τ to

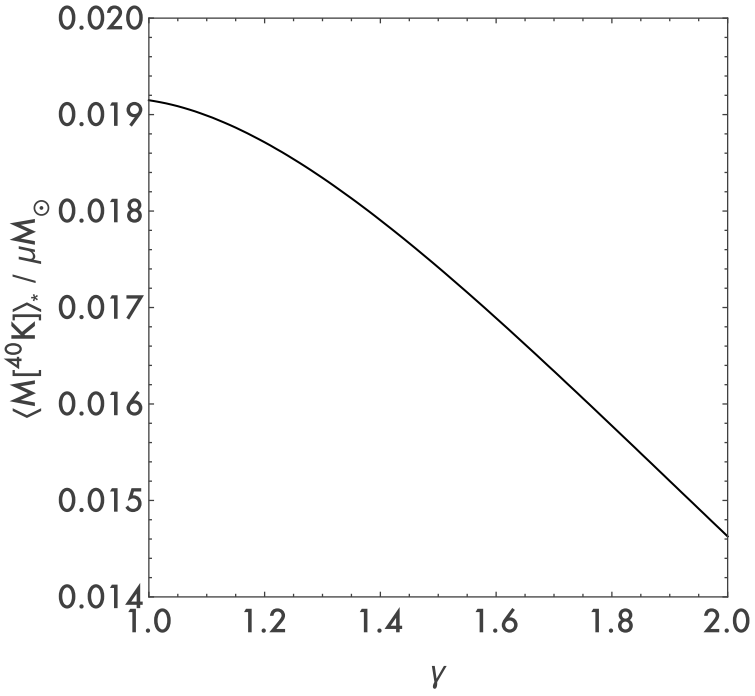

Fig. 3.— Radioactive yield per star for ^{40}K versus index γ of the stellar IMF. The yields, which are given in units of $\mu M_{\odot}$, are proportional to the fraction $\mathcal{F}_{SN}$ of stars above the supernova mass threshold, taken here to be 0.005.

a corresponding mass m_{min} by matching the evolutionary time of such a star to the cluster age, invoking the simple scaling law

$$\tau(\mathrm{Myrs}) = 3 + \frac{1200}{m^{1.85}} \,, \tag{6}$$

where this scaling law is consistent with detailed stellar evolution models (e.g., WW95, R02, and others) for stars massive enough to be supernova progenitors. If stellar disks lose the majority of their gas within 3 Myr, no enrichment can occur through the evolution and subsequent supernova explosion of a massive cluster member. On the other hand, disk survival times in excess of ~ 8 Myrs allow for the possibility of significant enrichment, owing to the fact that ^{40}K has a peak yield at $\sim 20 M_\odot$ (see Figure 1).

For the sake of definiteness, we use a minimum progenitor mass of 16 $M_\odot$ and an IMF index of $\gamma = 1.5$. This mass scale corresponds to a main-sequence lifetime of 10.1 Myr (see equation [6]), so that we are implicitly assuming that either circumstellar disks retain their mass over this time, or that they form after the progenitors. In this scenario, the fraction of stars that can enrich disks while they remain intact is

$$\mathcal{F}_\mathrm{c} = \mathcal{F}_\mathrm{SN} \, \frac{1.5}{8} \int_{16}^{\infty} \left(\frac{m}{8} \right)^{-2.5} dm = 0.0017 \,, \tag{7}$$

Studies of clusters out to 2 kpc (Lada & Lada 2003) and out to 1 kpc (Porras et al. 2003) indicate that in the solar neighborhood, the number of stars born in clusters with N members is (almost) evenly distributed logarithmically over the range $N \approx 30$ to 2000, with half of all stars belonging to clusters with $N \lesssim 300$. Clearly, stellar disks in small clusters have a small probability of being enriched as a result of a SN event within the cluster, whereas their couterparts in large clusters will likely be enriched from several SN events.

We now calculate enrichment distributions for stellar disk systems in the solar neighborhood. A typical stellar disk in a cluster will intercept a fraction

$$f(r) = \frac{\pi R_d^2}{4\pi r^2} \cos\theta \,, \tag{8}$$

of the radioactive yield produced by the entire cluster, where R_d is the disk radius, and r is the distance from the stellar disk to the cluster center (where the high-mass stars, and hence the supernova ejecta, originate). The factor of $\cos\theta$ takes into account the fact that the disk is not, in general, facing the supernova blast wave. For simplicity, we replace $\cos\theta$ with its mean value of 1/2. The radius r must be larger than the radius for which the disk (with radius R_d) is stripped due to the blast; for a disk of radius $R_d = 30$ AU, and for typical supernova energies, this minimum radial distance is $r_{min} \approx 0.1$ pc (Chevalier 2000; Ouellette et al. 2007; Adams 2010). The largest capture fraction expected is therefore $f_{max} \approx 2.6 \times 10^{-7}$. In turn, the maximum mass of ^{40}K that can be captured by a disk for a single SN event is found to be 65 p$M_\odot$ (p = 10^{-12}), although that requires an ideal progenitor mass of $M_* = 20 M_\odot$. More likely capture values for stellar disks located ~ 0.1 pc from a single progenitor would be ~ 0.1 p$M_\odot$, so distributions for local (Lada &

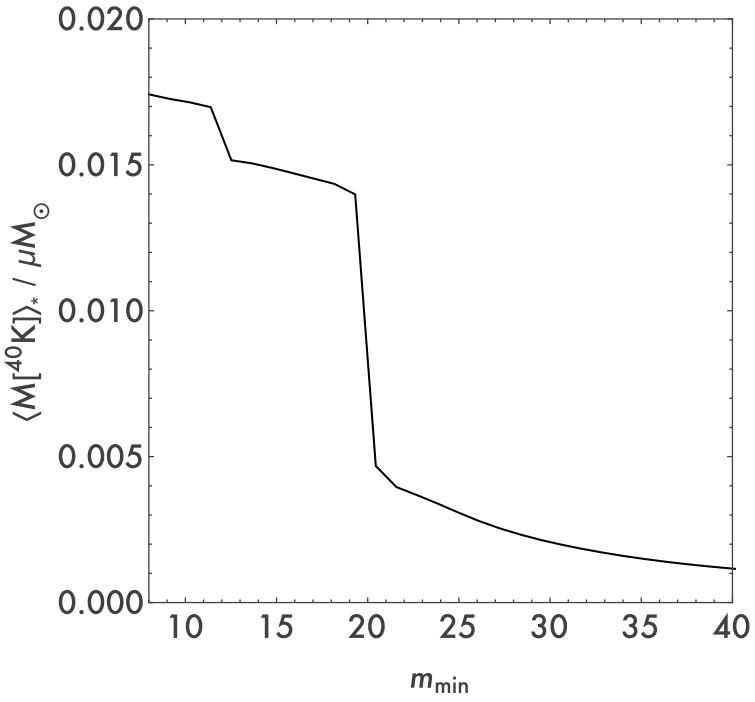

Fig. 4.— Radioactive yield per star for ^{40}K versus minimum mass of progenitor star included in the distribution for a stellar IMF with index $\gamma = 1.5$. The yields are given in units of $\mu M_\odot$, and are proportional to the fraction $\mathcal{F}_{SN}$ of stars above the supernova mass threshold, taken here to be 0.005.

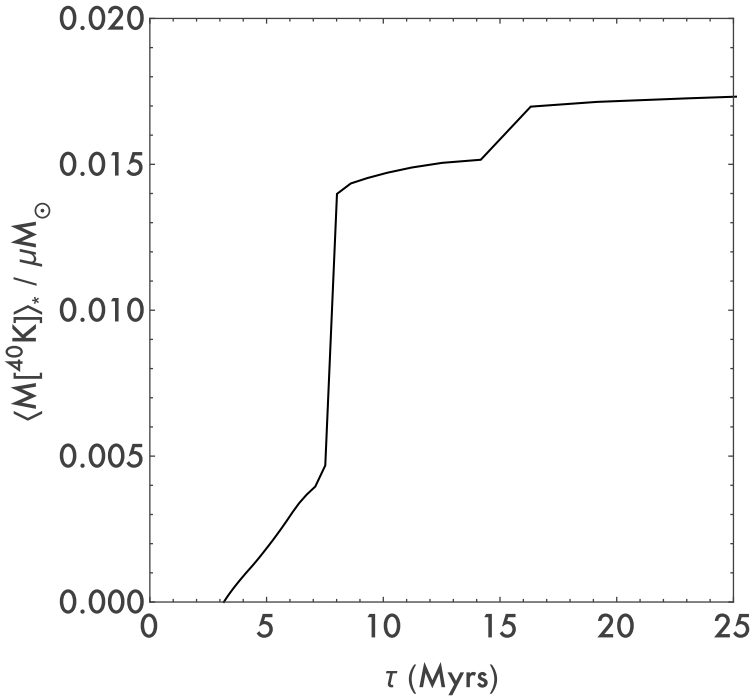

Fig. 5.— Radioactive yield per star for ^{40}K versus cluster age (in Myrs). For a given cluster age, only those stars that have evolved enough to explode as supernovae are included in the integral over the stellar mass distribution. The yields are given in units of $\mu M_{\odot}$ and the index of the stellar IMF is $\gamma = 1.5$. Yields are proportional to the fraction $\mathcal{F}_{SN}$ of stars above the supernova mass threshold, taken here to be 0.005.

Lada) clusters would be expected to range between $\sim 10^{-3}$ p$M_\odot$ and ~ 0.1 p$M_\odot$, with a high yield "wing" that extends up to $\sim 10^2$ p$M_\odot$.

To generate the distributions of captured mass, we first pick the cluster size that our "target" disk populates through a random sampling of a Lada & Lada cluster distribution, where the sampling uses a probability function that assigns the cluster size based on the probability of a star being in such a cluster (as opposed to the probability of a cluster having a given size). We then select the masses of each star within the cluster through a random sampling of the IMF, adopting a value of $\gamma = 1.5$ for our analysis. The cumulative yield of each isotope that results from the evolution of $\geq 16 M_\odot$ stars is then calculated, and assumed to originate from the cluster center. The location of a disk system is then randomly picked on the assumption that stars are distributed throughout the cluster in accordance to an average gas density profile $\rho_* \propto 1/r^\beta$, where observations indicate that β ranges between 1 and 2. We select a value of $\beta = 2$ in order to maximize the captured mass (since more stars are located near the cluster center), leading to the relation $dm \propto r^2 \rho_* dr \propto dr$. The cumulative probability that a star/disk system in a cluster with N members is located at radius r is then given by

$$P(r) = \left(\frac{r}{R_c} \right) , \tag{9}$$

where the outer boundary R_c is set through the empirically determined relation between cluster radius and number of stars

$$R_c(N) = 1 \, \mathrm{pc} \left(\frac{N}{300} \right)^{1/2} , \tag{10}$$

(see Figure 2 of Adams et al. 2006, which uses the data from Carpenter 2000 and Lada & Lada 2003). If the radius is smaller than 0.1 pc, the disk is assumed to not survive, and the result is not included in the distribution. Otherwise, the total yield from the progenitor stars is multiplied by the capture fraction f. The process is then repeated 100,000 times, with the resulting distribution presented in Figure 6. We then repeat the same process for a Lada & Lada type cluster distribution that extends up to $N = 10^6$, but adopt the more realistic large-cluster scaling

$$R_c(N) = 1 \, \mathrm{pc} \left(\frac{N}{300} \right)^{1/3} . \tag{11}$$

The resulting distribution is presented in Figure 7. We note that disks within the 0.1 pc disruption limit or for which no enrichment occurred are not represented in the histograms shown in Figures 6 and 7. For completeness, we present the percentages of stellar disk systems enriched by N_{SN} supernova events in Table 2 for both a local Lada & Lada distribution (LL) and for a Lada & Lada type cluster distribution that extends up to $N = 10^6$ (LL6). Only 43% of disk systems in a distribution of local (LL) clusters are expected to be enriched by at least one SN event, but that value increases to 77% for the extended (LL6) distribution (though in both cases a fraction of disks are destroyed because they are within the 0.1 pc limit). Even more dramatic, the mean value of SN explosions that enrich a disk system increases from 0.78 for the LL cluster distribution to 170 for the LL6 cluster distribution (note that the entries in Table 2 do not add up to 100 percent for the LL6 cluster distribution as many clusters have even larger numbers of supernovae).

Table 2. Percentage of disks enriched by N_{SN} events for local (LL) and extended (LL6) cluster distributions.

N_{SN}	% (LL)	% (LL6)
0	57	23
1	23	9.3
2	9.8	4.8
3	5.1	3.5
4	2.7	2.3
5	1.2	2.0
6	0.5	1.6
7	0.2	1.3

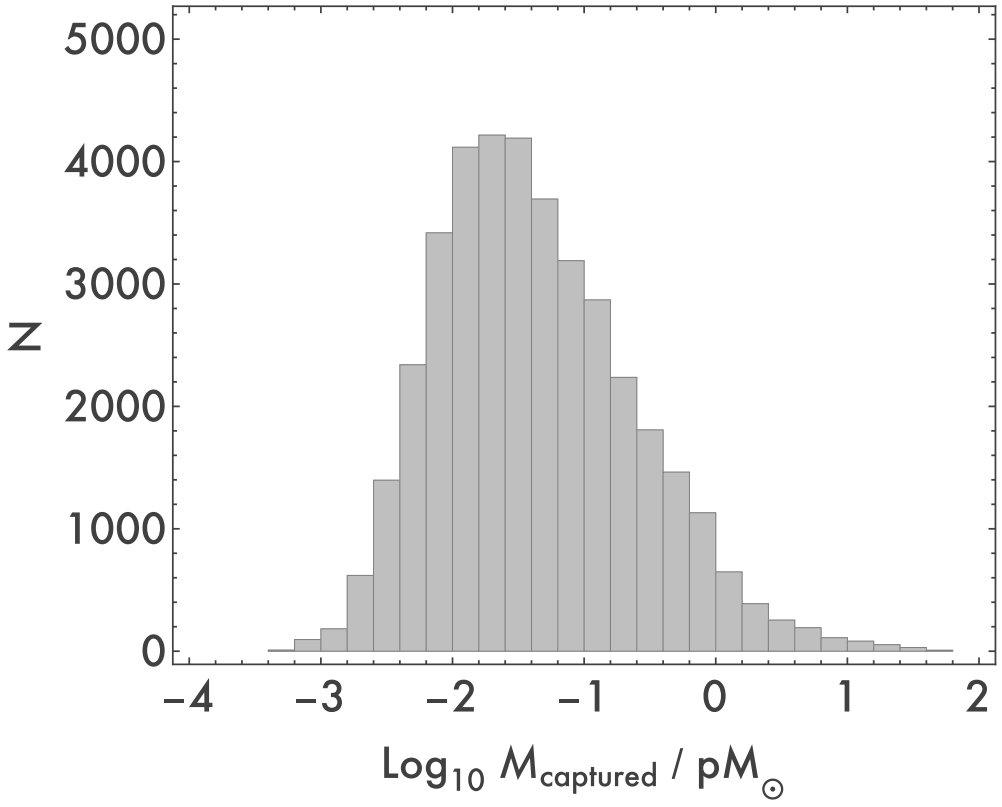

Fig. 6.— Histogram of the ^{40}K mass capture distribution for local clusters. Disk systems that were either distrupted because they were within 0.1 pc of the cluster center, or were not enriched due to a lack of SN events, are excluded from this distribution.

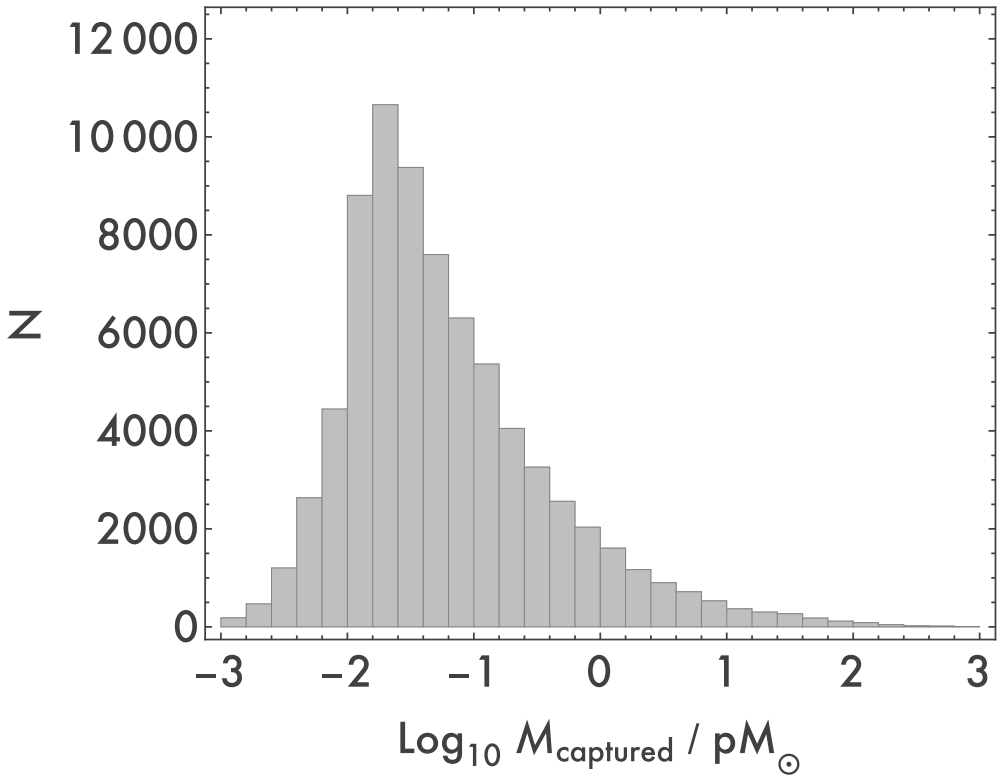

Fig. 7.— Histogram of the ^{40}K mass capture distribution for clusters that have a Lada and Lada distribution that extends to $N = 10^6$ stars. Disk systems that were either distrupted because they were within 0.1 pc of the cluster center, or were not enriched due to a lack of SN events, are excluded from this distribution.

To put our results in context, we estimate the mass of ^{40}K expected in a 30 AU disk given measured solar system abundances. Observations indicate that a 30 AU radius prototellar disk has a total mass of $\sim 0.02 M_\odot$ (e.g., Andrews et al. 2010), and a mass of hydrogen of $\approx 0.015 M_\odot$. Using the results from §2, we then find the corresponding expected mass of $M[^{40}\mathrm{K}]_{SS} \approx 140$ p$M_\odot$. The fraction of disks expected to be enriched at a level greater than $M_{SS}, 0.5M_{SS}, 0.1M_{SS}$ and $0.01M_{SS}$ under each scenario is given in Table 3, where LL denotes a Lada & Lada cluster distribution, and LL6 denotes the Lada & Lada distribution extended up to $N = 10^6$ stars. Note that these fractions are based on all systems sampled, including those that were not enriched or were destroyed (and are therefore not represented in the histograms of Figures 6 – 7). These results indicate that the fraction of systems that are enriched with ^{40}K yields at the level of our early solar system is about 0.005, or about 1 in 200. The corresponding fraction for enrichment at half (one tenth) of the solar system abundance is 0.009 (0.03). Although the fraction is low, the total number of systems in the Galaxy is large, with a corresponding large number of potentially habitable solar systems. If the prospects for habitability are enhanced by greater abundances of radioactive nuclei, then up to ~ 1 billion planets in the Galaxy could be enriched sufficiently to satisty this criteria.

4. Distributed Enrichment Scenarios

This section considers the case of distributed enrichment of radioactive nuclei, where the delivery of LLRs takes place over longer distances (and longer time scales) than direct enrichment within the cluster. Note that such enrichment can be considered over a range of size and time scales, and that the problem is not as well-defined as in the case of direct enrichment. Here we consider two cases: In the first scenario (§4.1), the supernovae from a given cluster can enrich the protostellar cores of a nearby cluster. In the second case (§4.2), we consider the entire molecular cloud as a dynamical system and consider the enrichment of LLRs over its lifetime. This latter scenario is more uncertain, but allows for greater radioactive enrichment.

Table 3. Fraction of disk enrichment by thresholds.

Case	LL	LL6	NN
$M > M[^{40}\mathrm{K}]_{SS}$	0	5.2×10^{-3}	1.3×10^{-2}
$M > 0.5M[^{40}\mathrm{K}]_{SS}$	0	9.2×10^{-3}	2.7×10^{-2}
$M > 0.1M[^{40}\mathrm{K}]_{SS}$	1.1×10^{-3}	3.0×10^{-2}	0.15
$M > 0.01M[^{40}\mathrm{K}]_{SS}$	1.3×10^{-2}	0.12	0.52

4.1. Neighboring Cluster Enrichment Scenario

In this section, we consider how much enrichment can occur in dense molecular cores whose parent cluster neighbors another cluster that evolved at an earlier time. To keep the analysis as simple as possible, we assume a fiducial core radius of $R_{core} = 0.1$ pc and core mass of $M_{core} = 10 M_{\odot}$. We also assume that all stars in the neighbor cluster with a mass $\geq 8 M_{\odot}$ evolve to their SN state before the cores in the parent cluster undergo collapse, and that the cores capture all of the radioactive isotopes that impinge upon them from the center of their neighboring cluster.

Ensuing distributions of capture mass are calculated by first selecting the neighbor cluster size (in terms of membership N) by sampling the local Lada & Lada cluster distribution (as was done in §3), and then sampling the IMF ($\gamma = 1.5$) to determine the mass of each star. The total mass yield ejected by stars massive enough to yield SN events is subsequently calculated using the yields as shown in Figure 1. The local Lada & Lada cluster distribution is then sampled again to determine the size of the parent cluster, and the radii of the neighbor cluster (R_{nc}) and parent cluster (R_{pc}) are set via the same scaling – as given by Equation (10) – that was used to set the cluster radius in §3 for the Lada and Lada cluster distribution. A molecular core is then placed at random in the parent cluster on the assumption that stars are distributed throughout the cluster in accordance to an average gas density profile $\rho_* \propto 1/r$. We note that setting $\beta = 1$ in the density profile (see discussion prior to Equation [9]) leads to a cumulative probability

$$P(r) = \left(\frac{r}{R_{pc}} \right)^2 , \tag{12}$$

that a core is located at radius r from the parent cluster center. As such, adopting this density profile distributes the highest fraction of cores near the cluster edge, and therefore maximizes the number of cores that have near maximum values of captured mass. The total mass captured by a core is then obtained by assuming that it is able to fully capture a fraction

$$f = \frac{\pi R_{core}^2}{4 \pi d^2} , \tag{13}$$

of the radioactive material ejected from the neigboring cluster, where the disance between the core and the neighbor cluster center

$$d = \sqrt{(R_{nc} + R_{pc} + R_{pc} \cos\theta_c)^2 + (R_{pc} \sin\theta_c)^2} , \tag{14}$$

is set through a random selection of the position angle θ_c. Results of the mass enrichment for the entire $10 M_{\odot}$ cores are shown in Figure 8 (in contrast, Figures 6 and 7 show mass enrichment for a 30 AU protostellar disk). For this scenario, 68% of cores sampled were enriched by at least one neighboring SN event – higher than the percentage of disk systems enriched for the local Lada and Lada cluster distribution because all stars with mass $\geq 8 M_{\odot}$ are assumed to lead to enrichment (as opposed to the $16 M_{\odot}$ limit assumed in §3). Cores for which no enrichment occurred are not represented in the histogram shown in Figure 8.

As a comparison, we estimate the mass of ^{40}K expected in a 10 $M_\odot$ core given measured solar system abundances. Using the isotope ratios from §2, we find the corresponding expected mass of $\approx 6.8 \times 10^4$ p$M_\odot$. Enhancement values are given in column NN of Table 3, where as with the LL and LL6 columns, fractions are based on all systems sampled, including those that were not enriched (and therefore not included in the histogram shown in Figure 8). Roughly 1% of solar systems are enriched with ^{40}K with radioactive yields comparable to those found in the early solar nebula. As discussed earlier, this fraction corresponds to billions of planets in a galaxy the size of our Milky Way.

4.2. Distributed Enrichment Scenario for entire Molecular Clouds

In this scenario we consider a molecular cloud as a star forming system and study the abundance of LLRs as a function of time. Let $M_{\rm c}$ denote the mass of the molecular cloud and let M_A denote the total mass contained in a given isotope of interest (e.g., ^{40}K).

The time evolution of the entire cloud is given by the equation

$$\frac{dM_{\rm c}}{dt} = -\Gamma_{\rm SF} - \dot{M}_c \,, \tag{15}$$

where $\Gamma_{\rm SF}$ is the star formation rate (in mass per unit time) and $\dot{M}_c$ is an additional mass loss term. Star formation is generally an inefficient process, such that only a fraction ϵ of the cloud mass is converted into stars over a free-fall time τ. In general, we can write the star formation rate in the form

$$\Gamma_{\rm SF} = \frac{\epsilon}{\tau} M_{\rm c} \,. \tag{16}$$

In the absence of the additional mass loss term $\dot{M}_c$, the molecular cloud mass would decay exponentially with decay time scale $T = \tau/\epsilon$. Since the free-fall time $\tau \sim 1$ Myr, and the efficiency is low, ϵ = 0.01 – 0.05, the decay time T = 20 – 100 Myr, which is roughly comparable to the expected cloud lifetimes. Without additional mass loss, the cloud would still retain 1/e of its original mass at the time when it should be destroyed. The additional term accounts for mass loss due to the disruptive effects of stellar winds and supernova explosions, i.e., feedback processes that act to dissipate the cloud. In this simple model, we parameterize the magnitude of the additional mass loss term by writing it in the form

$$\dot{M}_c = \gamma \frac{\epsilon M_{\rm c\,0}}{\tau} = \gamma \frac{M_{\rm c\,0}}{T} \,, \tag{17}$$

where $M_{\rm c\,0}$ is the initial mass of the cloud. With the mass loss terms specified through equations (16) and (17), the time evolution of the cloud mass can be determined,

$$M_{\rm c}(t) = M_{\rm c\,0} \left\{ (1+\gamma) \exp[-t/T] - \gamma \right\} \,. \tag{18}$$

Note that the cloud mass reaches zero at a time t_f given by

$$t_f = T \log \left[\frac{1+\gamma}{\gamma} \right] \,. \tag{19}$$

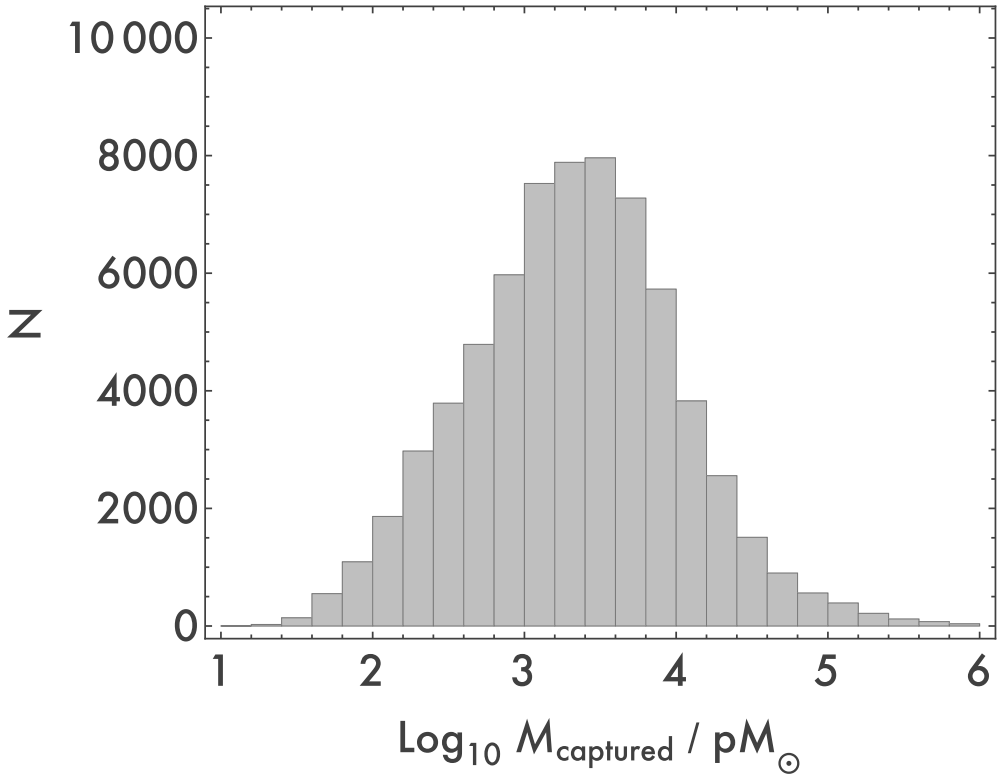

Fig. 8.— Histogram of ^{40}K mass capture distribution for the neighboring cluster scenario. These abundances represent the total mass captured by the core; only a fraction of this mass will be delivered to the nebular disk formed by its subsequent collapse. Molecular cores that were not enriched due to a lack of SN events in the neighboring cluster are excluded from this distribution.

The time t_f thus represents the total lifetime of the cloud. We can use observations to specify the cloud lifetime t_f and use equation (19) to determine the parameter γ, i.e.,

$$\gamma = \frac{1}{\exp[t_f/T] - 1} \approx \frac{1}{\mathrm{e} - 1} \approx 0.58\,. \tag{20}$$

The approximate values result from using a typical free-fall time $\tau = 1$ Myr, a star formation efficiency $\epsilon = 0.025$, and a cloud lifetime of $t_f = 40$ Myr, so that $t_f/T = 1$.

The time evolution of the mass in a given radioisotope is then given by the equation

$$\frac{dM_A}{dt} = \Gamma_{\mathrm{SF}} \frac{\langle M[A] \rangle_*}{\langle m \rangle} - \frac{M_A}{M_{\mathrm{c}}} \left[\Gamma_{\mathrm{SF}} + \gamma \frac{M_{\mathrm{c}\,0}}{T} \right] - \frac{\log 2}{t_{1/2}} M_A\,, \tag{21}$$

where $\langle M[A] \rangle_*$ is the mass of the isotope produced per star (averaged over the stellar IMF), and

$$\langle m \rangle = \int \frac{dN_*}{dm} m\, dm\,, \tag{22}$$

is the average stellar mass for a given IMF. For the isotopes of interest, the half-lives are of order 1 – 10 Gyr, whereas the cloud lifetimes are of order 0.1 Gyr, so we can ignore the third term in equation (21). The solution can be written in the form

$$M_A(t) = \left[M_{A0} + \frac{\langle M[A] \rangle_*}{\langle m \rangle} M_{\mathrm{c}\,0} \frac{t}{T} \right] \left\{ (1 + \gamma) \exp[-t/T] - \gamma \right\}\,. \tag{23}$$

The mass fraction $F_A(t)$ of the isotope A is thus given by

$$F_A(t) = \frac{M_A(t)}{M_{\mathrm{c}}(t)} = \left[\frac{M_{A0}}{M_{\mathrm{c}\,0}} + \frac{\langle M[A] \rangle_*}{\langle m \rangle} \frac{t}{T} \right]\,. \tag{24}$$

The mass fraction is thus a steadily increasing function of time. Note that the quantity $\langle M[A] \rangle_* / \langle m \rangle$ is essentially the mass fraction (of isotope A) produced by the aggegrate of supernovae in the cloud, whereas the quantity M_{A0}/M_{C0} is the starting mass fraction. We expect this second fraction to be smaller than the first. Moreover, the time t/T is of order unity near the end of the cloud's lifetime, so that the mass fraction increases toward the benchmark value

$$F_A(t) \rightarrow \frac{\langle M[A] \rangle_*}{\langle m \rangle}\,. \tag{25}$$

For the case of ^{40}K, for example, this asymptotic mass fraction is about 3.8×10^{-8}, which is about 5.6 times larger than early solar system abundance of the isotope (with a mass fraction of about 6.8×10^{-9} based on the Lodders 2010 values, as presented in Table 1). As a result, distributed enrichment over the course of a cloud's lifetime can – in principle – produce significant enrichment of long-lived radioactive nuclei.

The enrichment levels discussed above are subject to a number of uncertainties. This treatment of the problem implicitly assumes that all of the LLRs produced by supernovae remain in the

molecular cloud. In practice, however, some fraction will escape. In addition, the mass fraction only approaches its asymptotic value near the end of the cloud's lifetime, i.e., when it retains only a small fraction of its original mass. As a result, only the last generation of star formation within the cloud would be exposed to such high levels of radioactive nuclei. Since the mass fraction $F_A(t)$ is a linear function of time, the median enrichment level (in the absence of losses) is about half the asymptotic value, or about 3 times the cosmic abundance. Finally, we note that molecular clouds are complex and that supernova explosions are not uniformly distributed within the cloud. As a result, radioactive enrichment will not take place in a homogenous fashion.

5. Conclusion

This paper has considered the possible enrichment of circumstellar disks by long-lived radioactive nuclei, which are produced by supernovae in star forming regions.These LLRs are important components of the terrestrial planets that form within these disks. They provide a significant internal heat source that affects the internal structure of the planets, and helps to drive plate tectonics and related geophysical processes. This paper focuses of the isotope ^{40}K, because it is the most abundant and its production is relatively well understood (see also Table 1), and this section provides a summary of results (§5.1) and a discussion of their implications (§5.2).

5.1. Summary of Results

We have estimated the enrichment levels of ^{40}K from two different scenarios. In the first case, circumstellar disks are enriched directly by capturing ejecta from supernova explosions that detonate within the same clusters, and a range of possible distributions for the clusters are considered (see §3). For the most likely cluster distribution (a power-law distribution that extends up to stellar membership size $N = 10^6$), we find modest enrichment levels. Only about 1 in 200 solar systems are predicted to double the abundance of ^{40}K, whereas 1 in 30 systems should receive a 10% enhancement over the galactic background level. The typical enrichment levels of ^{40}K fall in the range 0.01 to 1 p$M_\odot$, with the tail of the distribution extending up to 100 p$M_\odot$ (see Figure 7).

In addition to direct enrichment, we have (briefly) considered two types of distributed enrichment. In one case, supernovae provide additional ^{40}K to the protostellar cores in a neighboring cluster (§4.1). Since the cores are extended, they can subtend larger solid angles (compared to circumstellar disks experiencing direct enrichment) in spite of their larger distances. This scenario is thus somewhat more effective than the case of direct enrichment. For example, about 1 in 80 solar systems are predicted to double their abundance of ^{40}K (see Table 3).

We have also considered the entire molecular cloud as a dynamical system (§4.2) and estimated the expected levels of enrichment of ^{40}K as the cloud evolves according to a simple model. In the absence of losses — assuming all of the ^{40}K produced by supernovae are retained within the cloud

— the later generations of star formation can be significantly enhanced in ^{40}K. The final generation could have radioactive abundances up to a factor of about 5 times that of the background galaxy. Only a relatively small fraction of the stars are produced at the end of the cloud's lifetime, however, so that most solar systems would be enhanced by smaller factors of $\sim 2-3$. When losses are included, these enrichment levels are even lower. Keep in mind that this global model is included for comparison, but has larger uncertainties than the calculations of direct enrichment (§3) or from neighoboring clusters (§4.1).

5.2. Discussion

The results of this paper have two important implications. The first is that the enrichment of long-lived radioactive nulcei (LLRs) is usually dominated by distributed enrichment mechanisms (rather than by direct enrichment within the birth clusters of forming solar systems). This finding is in contrast to the case of short-lived radioactive nuclei, where direct enrichment and distributed enrichment can provide roughly comparable amounts of SLRs (Adams et al. 2014). This result is not unexpected, since the long half-lives of LLRs allow them to travel much longer distances.

The second implication of this work is that the fraction of solar systems that experience substantial enrichment is of order one percent. Specifically, this claim holds for ^{40}K, which is one of the most important nuclear species for planetary structure. In this context, about one percent of solar systems receive enough LLRs to double their abundance compared to the galactic background. Although the neighboring cluster scenario is somewhat more effective (1 out of 80) than direct enrichment (1 out of 200), the results are roughly comparable, and the former case contains more uncertainties. Of course, doubling of the nuclear abundance only represents a useful benchmark for comparison; the full description of radioactive enrichment is provided by the distributions presented in §3 and §4.

We note that these nuclear enrichment scenarios become more uncertain as the distance from the supernovae (the source of LLRs) increases. For solar systems within the same cluster as the supernova explosion, we assume that the disks are efficient at capturing LLRs; in practice, however, some losses will occur. Additional losses arise due to timing issues, analogous to the case of SLR enrichment (Adams et al. 2014). For the neighboring cluster scenario, the abundances are calculated under the assumption of efficient capture and mixing over the entire core; additional calculations should explore the degree to which the captured LLRs are delivered to the planet-forming disks at the end of the star formation process. Some work along these lines has been carried out for the case of SLRs (see, e.g., Ouellette et al. 2009, 2010; Boss & Keiser 2015 and references therein), but this work should be generalized to the case of LLRs (where the time scales and length scales are different). Finally, distributed enrichment on the scale of the entire molecular cloud has much larger uncertainties than the other scenarios considered herein, and we have only considered a simple model for comparison (see also Gounelle & Meibom 2008, Gounelle et al. 2009 for a related treatment of SLRs). To carry this work forward, we need more realistic models of

molecular cloud evolution, as well as better observational constraints on their lifetimes.

Although only one percent of solar systems are predicted to experience substantial LLR enrichment, the total number of highly enriched systems in the Galaxy is quite large, of order 10^9. Since terrestrial planets are common, we expect a correspondingly large number of them to also be enriched: The first Earth-sized planet in the habitable zone of a main-sequence star has recently been detected (Quintana et al. 2014) and projections suggest that about 10 percent of Sun-like stars harbor Earth-like planets in habitable orbits (Petigura et al. 2013). Favorably enriched planets would have ample sources of internal heat, which helps to drive plate tectonics and other geophysical activity. It is possible that such planets could even be superhabitable, i.e., even more favorable for the development of life than our own Earth (Heller & Armstrong 2014). This possibility should be kept in mind as we continue the search for habitable worlds.

Acknowledgments: This paper benefited from discussions with many colleagues including Konstantin Batygin, Juliette Becker, Ilse Cleeves, Kate Coppess, Evan Grohs, Minyuan Kay, and Dave Stevenson. We thank the referee for useful comments. This work was supported at the University of Michigan through the Michigan Center for Theoretical Physics and at Xavier University through the Hauck Foundation.

REFERENCES

Adams, F. C. 2010, ARA&A, 48, 47

Adams, F. C., & Fatuzzo, M. 1996, ApJ, 464, 256

Adams, F. C., Fatuzzo, M., & Holden, L. 2014, ApJ, 789, 86

Adams, F. C., Proszkow, E. M., Fatuzzo, M., & Myers, P. C. 2006, ApJ, 641, 504

Andrews, S. M., Wilner, D. J., Hughes, A. M., Chunhua, Q., & Dullemond, C. P. 2010, ApJ, 723, 1241

Boss, A. P., & Keiser, S. A. 2015, arXiv:1507.03956

Buchave, L. A., Latham, D. W., Johansen, A. et al. 2012, Nature, 486, 375

Cameron, A.G.W., & Truran, J. W. 1977, Icarus, 30, 447

Carpenter, J. M. 2000, AJ, 120, 3139

Chabrier, G. 2003, PASP, 115, 763

Chevalier, R. A. 2000, ApJL, 538, L151

Cleeves, L. I., Adams, F. C., & Bergin. E. A. 2013, ApJ, 772, 5

Frank, E. A., Meyer, B. S., & Mojzsis, S. J. 2014, Icarus, 243, 274

Gonzales, G., Brownlee, D., & Ward, P. 2001, Icarus, 152, 185

Gounelle, M., & Meibom, A. 2008, ApJ, 680, 781

Gounelle, M., Meibom, A., Hennebelle, P., & Inutsuka, S-I. 2009, ApJ, 694, L1

Heller, R., & Armstrong, J. 2014, AsBio, 14, 50

Kasting, J. F., Whitmire, D. P., & Reynolds, R. T. 1993, Icarus, 101, 108

Kroupa, P. 2001, MNRAS, 322, 231

Lada, C. J., & Lada, E. A. 2003, ARA&A, 41, 57

Lodders, K. 2010, in Goswami A., Reddy B. E., eds, Principles and Perspectives in Cosmochemistry Solar System Abundances of the Elements. p. 379

Lunine, J. I. 2005, Astrobiology: A Multidisciplinary Approach (San Francisco: Pearson)

Mathews, G. J., Bazan, G., & Cowan, J. J. 1992, ApJ, 391, 719

Mishra, R., & Goswami, J. N. 2014, Geochim. Cosmochim. Acta, 132, 440

Ouellette, N., Desch, S. J., & Hester, J. J. 2007, ApJ, 662, 1268

Ouellette, N., Desch, S. J., Bizzarro, M., Boss, A. P., Ciesla, F., & Meyer, B. 2009, Geochim. Cosmochim. Acta, 73, 4946

Ouellette, N., Desch, S. J., & Hester, J. J. 2010, ApJ, 711, 597

Petigura, E. A., Howard, A. W., & Marcy, G. W. 2013, PNAS, 110, 19273

Porras, A., Christopher, M., Allen, L., et al. 2003, AJ, 126, 1916

Quintana, E. V., Barclay, T., Raymond, S. N. et al. 2014, Science, 344, 277

Rauscher, T., Heger, A., Hoffman, R. D., & Woosley, S. E. 2002, ApJ, 576, 323

Reddy, B. E., Tomkin, J., Lambert, D. L., & Prieto, C. A. 2003, MNRAS, 340, 304

Salpeter, E. E., 1955, ApJ, 121, 161

Scharf, C. A. 2009, Extrasolar Planets and Astrobiology (Mill Valley: Univ. Science Books)

Timmes, F. X., Woosley, S. E., & Weaver, T. A. 1995, ApJS, 98, 617

Umebayashi, T., & Nakano, T. 2009, ApJ, 690, 69

Woosley, S. E., & Weaver, T. A. 1995, ApJS, 101, 181

This preprint was prepared with the AAS LaTeX macros v5.2.